



## Research article

# miR-199a-5p targets DUSP14 to regulate cell proliferation, invasion and stemness in non-small cell lung cancer

Ying Zheng<sup>a</sup>, Chaokun Yang<sup>b</sup>, Shaoqiang Xie<sup>b</sup>, Desheng Liu<sup>b</sup>, Hui Wang<sup>b</sup>, Jinxin Liu<sup>b,\*</sup>

<sup>a</sup> Department of Anesthesiology, Yibin Second People's Hospital, No.96, North Street, Cuiqing District, Yibin City, 644000, PR China

<sup>b</sup> Department of Thoracic Surgery, Yibin Second People's Hospital, No.96, North Street, Cuiqing District, Yibin City, 644000, PR China

## ARTICLE INFO

## Keywords:

DUSP14  
miR-199a-5p  
Non-small cell lung cancer  
Proliferation  
Invasion  
Stemness

## ABSTRACT

**Background:** Non-small cell lung cancer (NSCLC) shows the highest morbidity among malignant tumors worldwide. Despite improvements of diagnosis and treatment, patient prognosis remains unfavorable. Therefore, there is a need to discover a novel treatment strategy for NSCLC. DUSP14 is related to various cancers as the regulatory factor for cellular processes. However, its specific roles in NSCLC and the upstream modulator remain largely unclear.

**Methods:** DUSP14 expression patterns within the lung cancer patient cohort from TCGA database were analyzed using UALCAN online tool. Different databases including miRDB, starbase, and Targetscan were employed to screen the upstream regulator of DUSP14. DUSP14 and miR-199a-5p expression was determined by qRT-PCR and Western blot techniques. To confirm binding interaction of DUSP14 with miR-199a-5p, we conducted a dual-luciferase reporter assay. Cell viability, migration, and stemness properties were assessed using CCK-8, EdU (5-ethynyl-2'-deoxyuridine) incorporation, transwell invasion, and sphere formation assays. The effect of DUSP14 silencing on tumorigenesis was assessed with the NSCLC cell xenograft mouse model.

**Results:** Our study discovered that DUSP14 exhibited high expression within NSCLC tumor samples, which is related to the dismal prognostic outcome in NSCLC patients. Silencing DUSP14 impaired NSCLC cell proliferation, migration, and tumor sphere formation. Besides, we identified miR-199a-5p as the upstream regulatory factor for DUSP14, and its expression was negatively related to DUSP14 level within NSCLC tissues. Introducing miR-199a-5p recapitulated the function of DUSP14 silencing in NSCLC cell aggressiveness and stemness. Moreover, knocking down DUSP14 efficiently inhibited tumor formation in NSCLC cells of the xenograft model.

**Conclusions:** Our study suggests that DUSP14 is negatively regulated by miR-199a-5p within NSCLC, whose overexpression is required for sustaining NSCLC cell proliferation, invasion and stemness.

## 1. Introduction

Non-small cell lung cancer (NSCLC) shows the highest morbidity among lung cancer subtypes, and it is recognized as the leading factor inducing cancer-associated deaths globally [1]. There are significant advancements and improvements in diagnosing and

\* Corresponding author. Yibin Second People's Hospital, No.96, North Street, Cuiqing District, Yibin City, 644000, PR China.  
E-mail address: [Liujinxin0852@163.com](mailto:Liujinxin0852@163.com) (J. Liu).

<https://doi.org/10.1016/j.heliyon.2024.e29102>

Received 31 October 2023; Received in revised form 31 March 2024; Accepted 1 April 2024

Available online 6 April 2024

2405-8440/© 2024 Published by Elsevier Ltd.

This is an open access article under the CC BY-NC-ND license

(<http://creativecommons.org/licenses/by-nc-nd/4.0/>).

treating NSCLC recently. Nonetheless, its global 5-year survival rate is still low at approximately 5 % when metastasis or recurrence occurs [2]. Therefore, it is crucial to search for novel biomarkers and investigate the mechanisms underlying the malignant progression to enhance the treatment and prognosis for NSCLC.

MicroRNAs (miRNAs) represent the endogenous non-coding RNAs responsible for regulating post-transcriptional gene levels [3]. They can bind to complementary sequences in 3' untranslated region (3'UTR) in target mRNAs, leading to mRNA translation inhibition or degradation [4]. Numerous studies have reported that miRNAs are important for tumor occurrence and development, like cell proliferation, apoptosis, migration, stemness, or other malignant processes [5,6]. miRNAs can play a role of oncogenes or tumor suppressors in NSCLC [7,8]. For instance, miR-199a-5p expression decreases within NSCLC, which is believed as the suppressor gene [9–12]. However, the mechanisms of miR-199a-5p in regulating the aggressiveness and malignant progression in NSCLC still require further investigation.

Dual-specificity phosphatases (DUSPs), proteins involved in regulating MAPK signaling pathway, are significant for tumor initiation, progression, and therapy resistance [13]. Recent studies have highlighted the significance of DUSP14 (called MAP-kinase phosphatase 6, MKP6 as well) in various pathophysiological conditions, including heart injury and cerebral ischemia-reperfusion injury [14,15]. Additionally, DUSP14 is discovered to show overexpression within pancreatic cancer to sustain malignant features in cancer cells [16]. Nevertheless, the functional relation of DUSP14 with NSCLC development remains unclear.

Here, the present work analyzed functional effects of DUSP14 on regulating NSCLC malignancy, and examined the interplay between DUSP14 and miR-199a-5p. Analysis of lung cancer patient cohort data from TCGA database revealed a high expression of DUSP14 within lung adenocarcinoma (LUAD) and lung squamous cell carcinoma (LUSC) samples. DUSP14 overexpression was related to the dismal prognostic outcome in cancer patients. Based on the above data, it is important to further analyze the functions of DUSP14 knockdown in NSCLC cell lines *in vitro* and *in vivo*. Moreover, we dissected functional interplay between miR-199a-5p and DUSP14 in dictating the aggressiveness and stemness of NSCLC cells.

## 2. Materials and methods

### 2.1. Human tissues and cell lines

Human NSCLC cells (A549, H1299, PC9, calu-3 and calu-6) as well as healthy human bronchial epithelial cells (BEAS-2B) were provided by American Type Culture Collection (ATCC, Manassas, VA, U.S.A.). Among them, A549, BEAS-2B and PC9 cells were cultivated within ATCC-formulated DMEM, H1299 cells were in RPMI-1640 and calu-3 and calu-6 cells were cultivated in MEM medium. Cells were cultivated under 37 °C and 5 % CO<sub>2</sub> conditions. The culture mediums of cells were added 10 % fetal bovine serum (FBS).

Tumor tissues and adjacent healthy tissues were collected from altogether 86 NSCLC patients undergoing surgical treatment at our hospital. The study protocol gained approval from the Ethics Committee of Yibin Second People's Hospital, Sichuan province, China (approval number: 20151216). Informed consent was obtained from every participant. The experiments involving human materials were performed following the World Medical Association Declaration of Helsinki.

### 2.2. Public data retrieval and analysis

We employed the UALCAN (<http://ualcan.path.uab.edu/analysis.html>) web-based approach to analyze lung cancer patient cohort data from TCGA database and evaluate DUSP14 expression within both lung cancer and non-carcinoma tissues [17]. The relations between DUSP14 levels in NSCLC patients and patient ages, genders, tumor sizes, tumor differentiation state, TNM grades, and lymph node metastasis were evaluated by Chi-square test. Additionally, the correlation between DUSP14 and miRNA-199a-5p expression levels in NSCLC tumor samples was assessed by Spearman's correlation method.

### 2.3. Transfection and preparation of the stable cells

DUSP14-specific short hairpin RNA (shRNA) and the scramble shRNA (sh-NC) were obtained from Dharmacon (Lafayette, USA), and inserted in pLKO.1 cloning vector. For DUSP14 overexpression, cDNA of human DUSP14 was inserted in pcDNA3.1 expression vector, with empty vector as the control. miR-199a-5p mimic (oligonucleotide Sequences: 5'-CCCAGUGU UCAGACUACCGUUC-3'; 5'-ACAGGUAGUCUGAACACUGGGUU-3') or negative control (mimics NC: 5'-UUCUCCGAACGUGUCACGUTT-3'; 5'-ACGUG ACACGUUCGGAGAATT-3') were purchased for Ambion (Austin, USA). By adopting Lipofectamine 2000 reagent (Invitrogen, USA), cells were subjected to another 48 h transfection using 6 µg shRNA plasmid or 100 nM miRNA mimic. To select for cells stably expressing DUSP14-targeting shRNA, cells under pLKO.1-sh-DUSP1 or pLKO.1-sh-NC transfection were cultured using 600 µg/mL G418 (Sigma, Germany) for 10 days until resistant cell clones emerged. The cell clones were expanded in the medium with 200 µg/mL G418 as the stable cells.

### 2.4. Cell Counting Kit-8 (CCK-8) assay

PC9, A549 and H1299 cells (2500/well) were seeded into 96-well plates. The cells were cultivated at 37 °C until 72 h. All wells were added with CCK-8 reagent (10 µl, Beyotime, Beijing, China) at 24, 48 and 72 h and incubated for another 2 h under 37 °C. Next, absorbance values were detected using Synergy H1 microplate reader (BioTek, CA, USA) at 450 nm.

## 2.5. EdU incorporation assay

Cells with different treatments ( $5 \times 10^5$ /well) were inoculated in 6-well plate. This assay was conducted using the Click-iT™ EdU Cell Proliferation Kit for Imaging (Thermo Fisher Scientific, USA). After pulse-labeling with 1X EdU solution for 2 h, cells were rinsed by PBS twice and fixed using 3.7 % formaldehyde at room temperature for 15 min. Then, cells were rinsed again prior to 20-min 0.5 % Triton® X-100 treatment and another 30-min incubation using 1 x Click-iT® reaction cocktail. After removing staining solution, cells were rinsed by PBS twice. Then, DAPI (500 nM) was added for counter-staining, and a Leica AM6000 microscope (Leica, Germany) was employed for capturing cellular images.

## 2.6. Real-time quantitative PCR (qRT-PCR)

TRIZOL reagent (Invitrogen, USA) was utilized to extract total cellular and tissue RNAs, which were subsequently prepared to cDNA using QuantiTect Reverse Transcription Kit (QIAGEN, Germany) through reverse transcription. For microRNA quantification, cDNA was prepared from total RNA by the Taqman™ microRNA reverse transcription kit (Thermo Fisher Scientific, USA). QuantiNOVA SYBR Green PCR Kit (QIAGEN, Germany) was also utilized for qPCR according to the provided instructions. Primer sequences adopted for qPCR analysis included: DUSP14: 5'-TCAACTGGCCCAATTTGAGT-3' (forward, F); 5'-CATCAGGTACGCGATACACAG-3' (reverse, R); GAPDH: 5'-TATGATGAT ATCAAGAGGGTAGT-3' (F); 5'-TGTATCCAACTCATTGTCATAC-3' (R). has-miR-199a-5p: 5'-CGCGCCAGTGTTCAGACTAC-3' (F); 5'-AGTGCAGGGTCCGAGTATT-3' (R); U6: 5'-CTCGCTTCG GCAGCACA-3' (F); 5'-AACGTT-CACGAATTTGCGT-3' (R). The  $2^{-\Delta\Delta Ct}$  approach was employed for determining relative gene expression, with GAPDH and U6 being endogenous references for DUSP14 and miR-199a-5p, separately.

## 2.7. Western-blotting

RIPA lysis buffer containing protease inhibitors (Beyotime, Beijing, China) was utilized to lyse cells and tissues. Thereafter, a BCA assay kit (Beyotime, Beijing, China) was utilized for determining protein content. Protein aliquots were then isolated through SDS-PAGE prior to transfer on a PVDF membrane. After 1-h blocking with BSA, the membrane was subsequently incubated overnight at 4 °C using primary antibodies (antibodies against DUSP14, SOX2, OCT4, or GAPDH, at a dilution of 1:1000, Abcam, UK). After membrane washing, secondary detection antibodies were applied for 1 h under ambient temperature, while the enhanced ECL Chemiluminescence kit (Beyotime, Beijing, China) was adopted for protein band signal development. The ChemiDoc Touch Imaging System (Bio-Rad, USA) was utilized for protein band imaging, whereas ImageJ software (NIH, USA) was applied in quantification.

## 2.8. Transwell invasion assay

After trypsinization, we harvested NSCLC cells within the serum-free medium. After coating Matrigel (BD Biosciences, USA) onto the top Transwell chamber (Corning, USA) for 15 min at 37 °C,  $2 \times 10^5$  cells were seeded into the upper compartment, whereas the bottom chamber was introduced with 20 % serum-containing medium (500  $\mu$ L). At 24 h later, 4 % paraformaldehyde was introduced for fixing invading cells for a 10-min period under ambient temperature, followed by 20-min staining using 0.1 % crystal violet (Sigma, Germany). The invading cells were imaged and quantified in 5 random fields for every sample at 200x magnification with the light microscope (Olympus, Japan).

## 2.9. Sphere formation assay

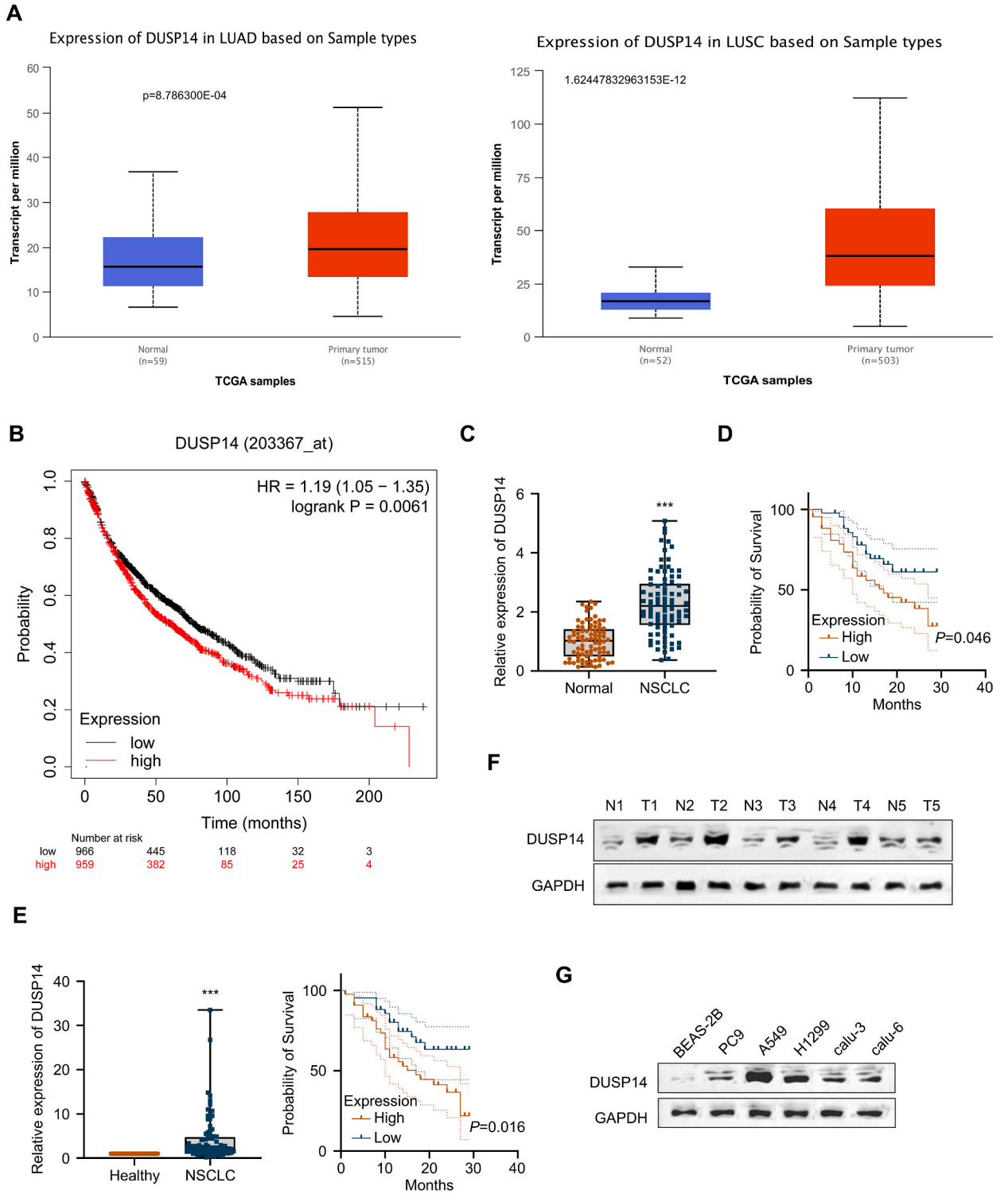
Tumor spheroids were generated by inoculating NSCLC cells ( $2 \times 10^3$ /well) into Matrigel-coated U-bottom 96-well plates. The cells were cultivated for 3–5 days at 37°C and 5 % CO<sub>2</sub> until individual spheres were observed. The number of spheroids was quantified with the bright-field microscope (Olympus, Tokyo, Japan).

## 2.10. miRNA identification

For identifying miRNA regulators for DUSP14, the three online miRNA resources (miRDB, starbase and Targetscan) were used to predict potential miRNA candidates for DUSP14 mRNA. The analysis revealed 6 common miRNAs (hsa-miR-199a-5p, hsa-miR-199b-5p, hsa-miR-873-3p, hsa-miR-430b-5p, hsa-miR-155-5p, hsa-miR-589-5p) with candidate binding sites within 3'UTR in DUSP14 mRNA.

## 2.11. Dual-luciferase reporter assay

Fragment of predicated wild-type binding site (WT) or mutated sequences (MUT) was inserted in PmirGLO Firefly luciferase reporter (Promega, USA). Afterwards, NSCLC cells were co-transfected with reporter vector or Renilla luciferase control plasmid and miRNA mimic or miR-NC (negative control). At 48 h post-transfection, relative Firefly/Renilla luciferase activities were determined using a One-Step Firefly Luciferase Assay Kit (Biovision, USA).



(caption on next page)

**Fig. 1. Elevated DUSP14 expression is related to a poor prognosis in NSCLC patients.** A. DUSP14 expression levels in NSCLC and LUSC patient cohort from TCGA database were analyzed using online tool UALCAN. The dataset included 515 LUAD tumor tissues, 503 LUSC tissues, and the matched normal tissues. B. Kaplan-Meier curve analysis of the overall survival of lung cancer patients between the DUSP14 high-expression and low-expression groups. C. qRT-PCR detection of DUSP14 expression in the clinical samples NSCLC tumor tissues and normal tissues (n = 86 pairs). D. Kaplan-Meier curve analysis of the overall survival in NSCLC patients based on the median value of DUSP14 expression in tumor tissues. E. Kaplan-Meier curve analysis of the overall survival in NSCLC patients according to the median value of DUSP14 expression in tumor tissues which were normalized against the matched normal control tissues. F. Expression of DUSP14 in normal tissues and NSCLC tissues were examined by Western blot (n = 5 pairs, N = normal; T = Tumor). G. Expression of DUSP14 in normal human bronchial epithelial cell line (BEAS-2B) and NSCLC cell lines (A549, H1299, PC9, calu-3, and calu-6). GAPDH acted as an internal control. Data is shown to be mean  $\pm$  SD of three biological replicates. \*\*\* $p < 0.001$ , compare to normal tissues.

## 2.12. Animal experiments

Our animal experimental protocols gained approval from the Institutional Animal Care and Use Committee at Yibin Second People's Hospital, Sichuan Province, China. For establishing a BALB/c nude mouse model of NSCLC xenograft, we transfected  $1 \times 10^7$  A549 cells with stable transfection using sh-NC or DUSP14 shRNA (sh-DUSP14) in right flank in mice. The tumor volume and body weight were recorded at 7-day intervals for 5 weeks. Tumor volume was determined by  $(\text{length} + \text{width}^2)/2$ . At 35 days later, each mouse was given euthanasia with CO<sub>2</sub> asphyxiation and terminal death was ensured by cervical dislocation. Tumor tissue was harvested for further analyses.

## 2.13. Immunohistochemistry

Paraformaldehyde-fixed tumor samples were processed into 5  $\mu\text{m}$  sections. The tumor sections were then deparaffinized with xylene and re-hydrated in distilled water. The sections were heated within the citrate unmasking solution (Beyotime, Beijing, China) for 15 min at 98  $^{\circ}\text{C}$  for antigen retrieval. After cooling for 30 min, the section was subjected to 10-min inactivation using 3 % hydrogen peroxide. Then, sections were rinsed thrice with PBS, and blocked using 5 % normal goat serum under ambient temperature for 1h. The tissue sections were later subjected to incubation using anti-DUSP14 or anti-Ki67 antibody (1: 500, Abcam, UK) under 4  $^{\circ}\text{C}$  for 18 h, followed by the labeling using a secondary antibody conjugated with horseradish peroxidase (1:2000, Abcam, UK). The signal development was performed for 3–5 min using a DAB Detection kit (Abcam, UK).

## 2.14. Statistical analysis

Every assay was conducted thrice. Results were represented by mean  $\pm$  SD. GraphPad Prism 8.0 (GraphPad software, USA) was utilized to analyze data, and between-group differences were statistically assessed by one-way ANOVA and Student's t-test.  $p < 0.05$  stood for statistical significance for all data analyses.

## 3. Results

### 3.1. Elevated DUSP14 expression is related to a dismal prognostic outcome of NSCLC patients

Clinical relevance of DUSP14 was evaluated through analyzing the TCGA Lung cancer patient cohort using UALCAN, an online database that provides comprehensive cancer transcriptome information. The dataset included 515 LUAD tumor tissues, 503 LUSC tissues, and the matched normal tissues. The analysis revealed that tumor tissues expressed higher levels of DUSP14 compared to normal counterparts (LUAD:  $p = 8.786300\text{E-}04$ ; and LUSC:  $p = 1.62447832963153\text{E-}12$ ) (Fig. 1A). Additionally, as revealed by Kaplan-Meier survival curve, patients showing DUSP14 up-regulation exhibited a poor overall survival compared to patients having lower DUSP14 levels (Fig. 1B). To validate these findings, we performed qRT-PCR for measuring DUSP14 levels within 86 paired NSCLC and non-carcinoma tissues. As expected, DUSP14 expression markedly increased within NSCLC tissues in comparison with adjacent non-carcinoma counterparts ( $p < 0.001$ ) (Fig. 1C). According to median DUSP14 expression in tumor samples, we grouped patients as high- or low-expression group. The overall survival rate was significantly higher among low-expression patients than high-expression counterparts ( $p < 0.05$ ) (Fig. 1D). We further normalized DUSP14 expression level in the tumor samples against that of the matched normal tissues, and then divided the patients as low- or high-expression group based on median normalized DUSP14 expression. Similar results were observed for the reduced overall survival rate among high-expression patients ( $p < 0.05$ ) (Fig. 1E). Based on the above data, DUSP14 overexpression is related to a dismal prognosis in NSCLC patients. DUSP14 protein expression also increased within NSCLC tumor tissues, as revealed by Western-blotting assay ( $p < 0.001$ ) (Fig. 1F). DUSP14 expression was also elevated in NSCLC cells (A549, H1299, PC9, calu-3, and calu-6) when compared to healthy human bronchial epithelial cells BEAS-2B (Fig. 1G).

To gain more insights into the relevance of DUSP14 expression to the clinical features of NSCLC patients, we classified 86 NSCLC patients as high- or low-expression group and explored the relationship between DUSP14 expression and clinicopathological data of NSCLC patients through Chi-square test. We found that DUSP14 expression level showed positive relation to tumor size, differentiation, TNM stage, and lymph node metastasis ( $p < 0.001$ ); but not to patient's age and gender (Table 1). Thus, DUSP14 upregulation is probably related to NSCLC malignant progression.

### 3.2. Knocking down DUSP14 suppresses NSCLC proliferation, invasion and stemness

Given that DUSP14 was highly expressed within NSCLC cells and tissues, it was hypothesized that DUSP14 may contribute to NSCLC malignant progression. For investigating DUSP14's role, we stably transfected NSCLC cells (PC9, H1299 and A549) with sh-NC or DUSP14 shRNA (sh-DUSP14). The knockdown efficiency of DUSP14 was analyzed through Western-blotting, which revealed that sh-DUSP14#1 had the strongest silencing effect (Fig. 2A). CCK8 experimental data indicated that DUSP14 shRNA#1 significantly impaired the proliferation of NSCLC cells (Fig. 2B). Consistently, EdU incorporation assay showed a reduced DNA synthesis in NSCLC cells with DUSP14 knockdown (Fig. 2C). Furthermore, silencing DUSP14 attenuated the invasion ability (Fig. 2D), and suppressed the sphere growth of NSCLC cells (Fig. 2E). Additionally, expression of SOX2 and OCT4 was evaluated by Western-blotting. DUSP14 knockdown reduced SOX2 and OCT4 expression within NSCLC cells (Fig. 2F). These findings collectively suggest that DUSP14 exerts the significant effect on modulating NSCLC cell growth, invasion, and the stemness.

### 3.3. miR-199a-5p shows negative regulation on DUSP14 expression

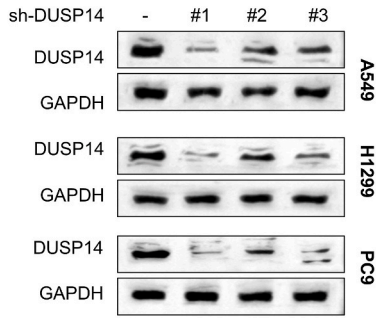
miRNA is capable of complementary binding to 3'UTRs in mRNA targets to regulate their degradation or translation. In order to shed more lights on the DUSP14 regulatory mechanism in NSCLC, we conducted bioinformatics analyses to identify potential miRNA regulators of DUSP14. Using three miRNA prediction tools, we identified six candidate miRNAs that share complementary binding sequence to DUSP14 mRNA: hsa-miR-199a-5p, hsa-miR-199b-5p, hsa-miR-873-3p, hsa-miR-430b-5p, hsa-miR-155-5p, and hsa-miR-589-5p (Fig. 3A). Subsequently, we measured DUSP14 expression within NSCLC cells transfected with mimic for each miRNA. Among the six miRNA mimics, there was a significant downregulation of DUSP14 mRNA after introducing miR-199a-5p mimic into both H1299 and A549 cells (Fig. 3B). There was the miR-199a-5p binding site on 3'UTR in DUSP14 mRNA, as predicted via TargetScan online tool (WT sequence), and the corresponding mutations introduced (MUT) was displayed in Fig. 3C. For confirming the interaction of DUSP14 with miR-199a-5p, we conducted a luciferase reporter assay. A WT DUSP14 luciferase reporter or the MUT that lacked candidate miR-199a-5p binding sites was co-transfected with miR-NC (negative control for miRNA mimic) or miR-199a-5p mimic into A549 and H1299 cells. As a result, miR-199a-5p mimic dramatically repressed WT reporter activity, but it did not inhibit MUT reporter (Fig. 3D), indicating that miR-199a-5p interacted with DUSP14 mRNA via predicted binding sites. Moreover, miR-199a-5p mimic decreased DUSP14 protein expression within NSCLC cells (Fig. 3E). In the clinical samples, miR-199a-5p expression dramatically decreased in NSCLC tissues relative to the matched normal tissues (Fig. 3F). As revealed by Spearman correlation analysis, DUSP14 was negatively correlated with miR-199a-5p levels within NSCLC tissues (Fig. 3G). Collectively, miR-199a-5p exerts negative regulation on DUSP14 expression in NSCLC.

**Table 1**

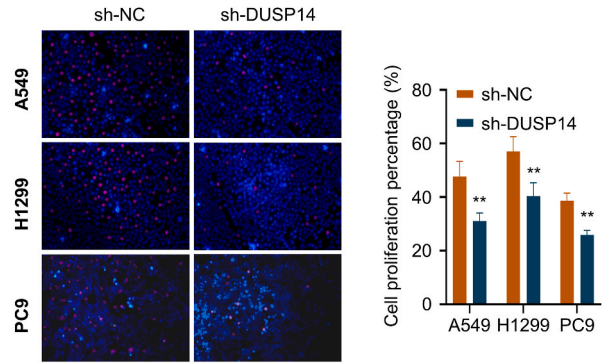
Association between DUSP14 expression and clinicopathological features of patients with non-small cell lung cancer.

Characteristics	Total	Low DUSP14 expression (n = 43)	High DUSP14 expression (n = 43)	P value
Age (years)				0.28
<60	45	25	20	
≥60	41	18	23	
Gender				0.666
Male	44	23	21	
Female	42	20	22	
Size (cm)				0.033
<4	61	35	26	
≥4	25	8	17	
TNM stage				0.031
I-II	46	28	18	
III-IV	40	15	25	
T stage				0.01
T1-T2	46	29	17	
T3-T4	40	14	26	
Differentiation				0.043
Well/moderate	55	32	23	
Poor/not	31	11	20	
Lymph node metastasis				0.037
N0-N1	59	34	25	
N2-N3	27	9	18	
Distant metastasis				0.041
M0	66	37	29	
M1	20	6	14	
Tumor location				0.131
Left	41	24	17	
Right	45	19	26	

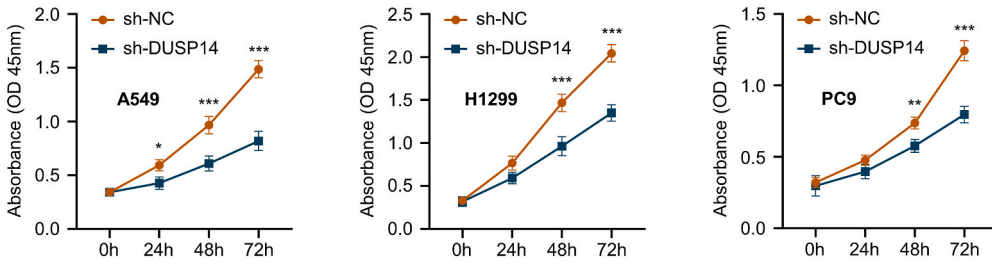
**A**



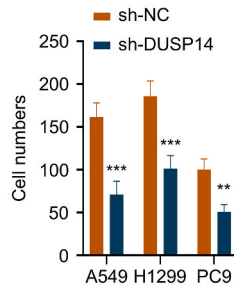
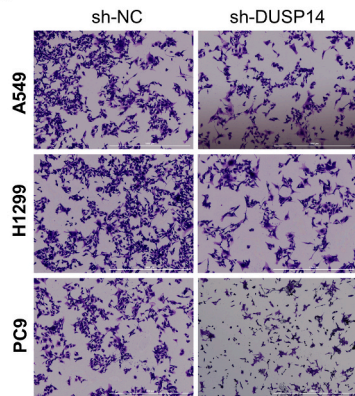
**C**



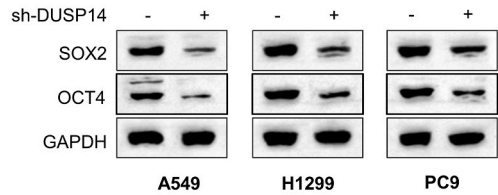
**B**



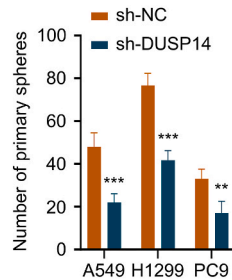
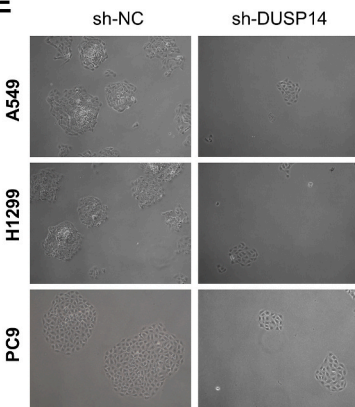
**D**



**F**



**E**



(caption on next page)

**Fig. 2. Knocking down DUSP14 inhibits the proliferation, invasion and stemness of NSCLC cells.** In order to investigate the function of DUSP14, three NSCLC cell lines (PC9, H1299 and A549 cells) were stably transfected with plasmid expressing control shRNA (sh-NC) or DUSP14 shRNA (sh-DUSP14). **A.** The knockdown efficiency of DUSP14 was examined using Western blot. **B.** CCK8 assay measurement of the cell growth rates at 24, 48 or 72h in sh-NC and sh-DUSP14 groups. **C.** EdU incorporation assay in sh-NC and sh-DUSP14 groups. **D.** Transwell invasion assay in sh-NC and sh-DUSP14 groups. **E.** Sphere formation assay in sh-NC and sh-DUSP14 groups. **F.** The expression levels of stem cell markers (SOX2 and OCT4) were measured by Western blot. All experiments were repeated three times, quantitative data was shown as mean ± SD. \* $p < 0.05$ , \*\* $p < 0.01$  and \*\*\* $p < 0.001$  relative to NC shRNA.

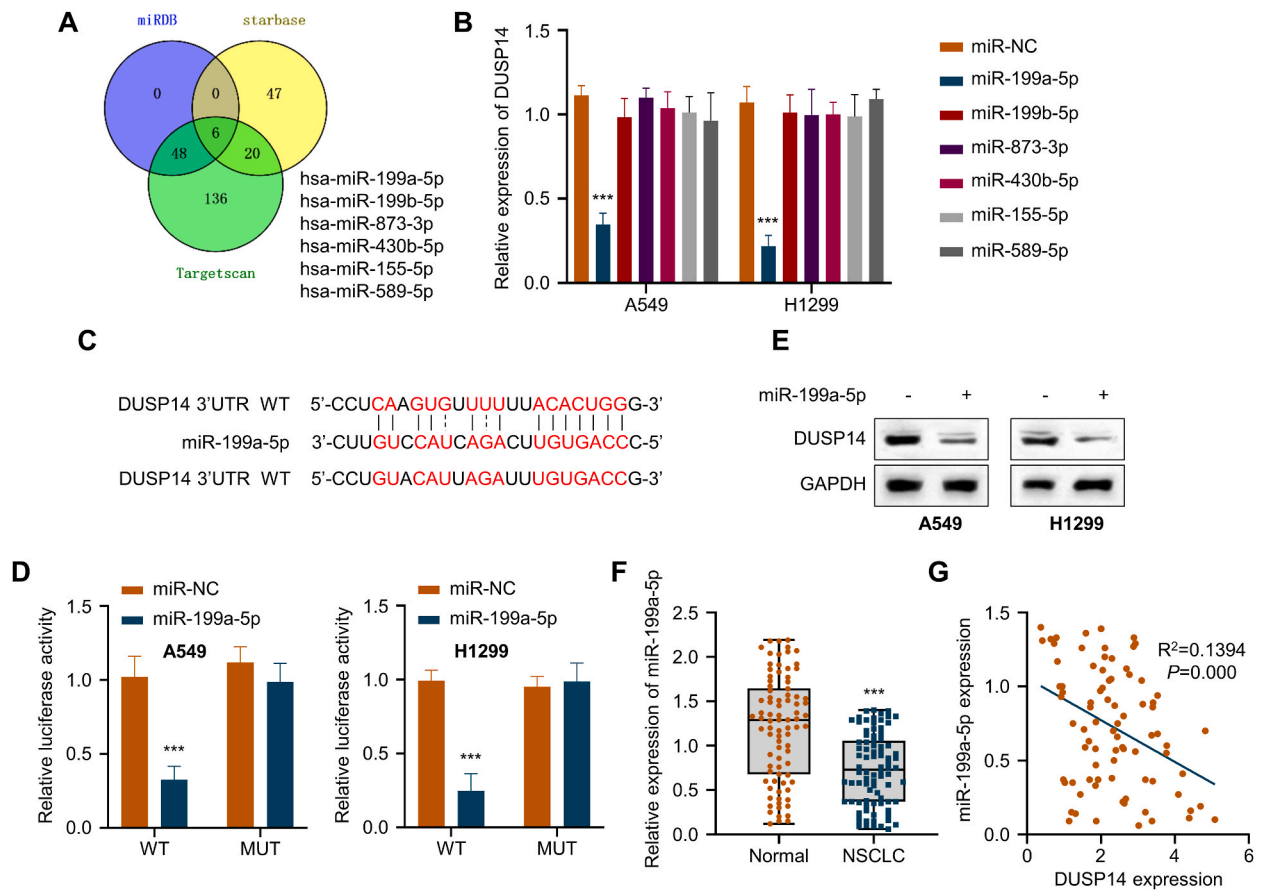


**Fig. 3. miR-199a-5p negatively regulates DUSP14 expression.** **A.** Six potential miRNA regulators of DUSP14 were produced by three online tools (miRDB, starbase and Targetscan). **B.** qRT-PCR was used to identify the DUSP14 mRNA levels after miRNA mimic transfection. **C.** Schematics of miR-199a-5p putative binding site in the 3' UTR of DUSP14 mRNA and the corresponding mutated sequence. **D.** Luciferase reporter assay in NSCLC cells using DUSP14 wildtype or mutated reporter in the presence of either miR-NC or miR-199a-5p mimic. **E.** A549 and H1299 cells were transfected with miR-199a-5p mimic or miR-NC, and Western blot was adopted for measuring DUSP14 protein levels. GAPDH served as an internal control. **F.** qRT-PCR analysis of miR-199a-5p levels in NSCLC tumor tissues and normal counterparts (n = 86 pairs). **G.** Spearman correlation analysis of DUSP14 and miR-199a-5p expression levels in NSCLC tissues. Data was expressed to be mean ± SD of three biological replicates. \*\*\* $p < 0.001$ , miR-199a-5p mimic compared with NC mimic, NSCLC compared to normal tissues.

**3.4. DUSP14 is a downstream modulator for miR-199a-5p in regulating NSCLC cell malignancy**

Since miR-199a-5p targets DUSP14 in NSCLC cells, we wondered whether miR-199a-5p/DUSP14 axis modulates malignant phenotype of NSCLC cells. To this end, we constructed DUSP14-expressing plasmid, which could promote the protein level of DUSP14 in both A549 and H1299 cells (Fig. 4A). Then, A549 and H1299 cells were transfected with miR-NC, miR-199a-5p mimic and empty vector or miR-199a-5p mimic plus DUSP14-expressing plasmid. The transfection of miR-199a-5p mimic notably impair the cell growth of NSCLC cells, as demonstrated by the CCK-8 and EdU incorporation assays; however, the inhibitory impact was partially rescued by DUSP14 overexpression (Fig. 4B and C). Transwell assay revealed that miR-199a-5p mimic inhibited the invasion of NSCLC cells, whereas DUSP14 overexpression promoted the invasive capability (Fig. 4D). Similarly, miR-199a-5p mimic suppressed sphere formation in NSCLC cells, which was rescued upon the overexpression of DUSP14 (Fig. 4E). We further indicated that DUSP14 overexpression could upregulate the protein levels of SOX2 and OCT4 in NSCLC cells with miR-199a-5p mimic transfection (Fig. 4F). The



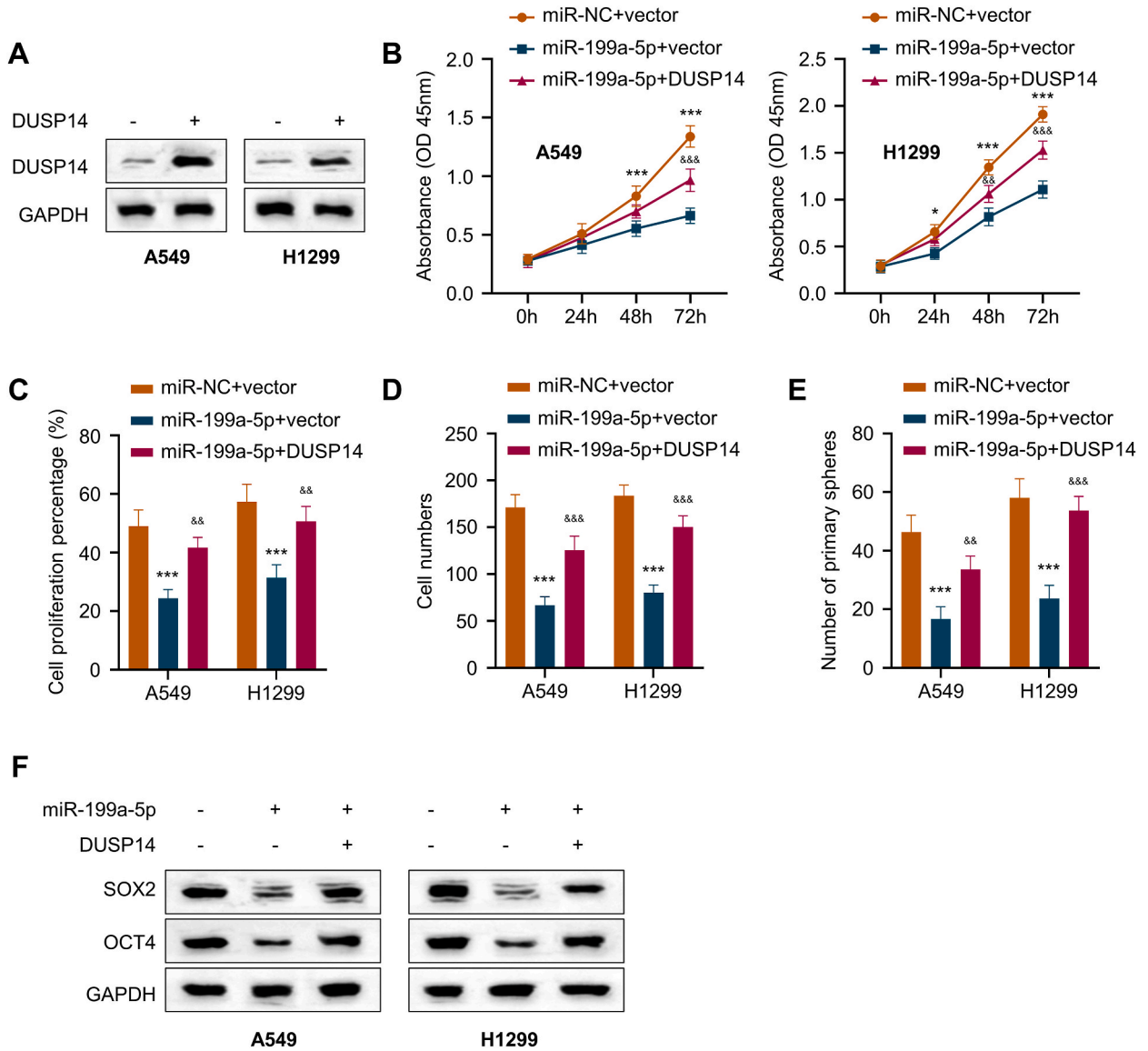


**Fig. 4.** DUSP14 is a downstream modulator of miR-199a-5p in regulating the malignancy of NSCLC cells. A549 and H1299 cell were transfected with miR-NC + empty vector, miR-199a-5p mimic and empty vector, or miR-199a-5p mimic and DUSP14 expression plasmid **A**. Western blot detection of DUSP14 protein levels after the transfection with DUSP14 expression plasmid. **B**. CCK8 assay measurement of the cell growth rates at 24, 48 or 72h in each experimental group. **C**. EdU incorporation assay in each experimental group. **D**. Transwell invasion assay in each experimental group. **E**. Sphere formation assay in each experimental group. **F**. The expression levels of stem cell markers (SOX2 and OCT4) were measured using Western blot. Data were shown to be mean  $\pm$  SD of three independent experiments,  $***p < 0.001$ ,  $**p < 0.01$  and  $*p < 0.05$ , relative to miR-NC + empty vector;  $***p < 0.001$ ,  $**p < 0.01$  and  $*p < 0.05$ , relative to miR-199a-5p + empty vector.

obtained results imply that miR-199a-5p represses DUSP14 expression to impair the aggressiveness of NSCLC cells.

### 3.5. DUSP14 is required of the tumor growth of A549 cells in vivo

To verify the functional engagement of DUSP14 in tumor formation, A549 cells stably expressing sh-NC or sh-DUSP14 were subject to injection into BALB/c nude mice. The body weight and the tumor volume were measured every seven days for 5 weeks. We did not find significant difference in the body weight between the two groups of mice (Fig. 5A). A549 cells with DUSP14 knockdown showed retarded tumor growth compared to the control cells expressing sh-NC (Fig. 5B and C). In the tumor tissues from A549 cells with DUSP14 knockdown, there was decreased expression of cell proliferation marker Ki67 (Fig. 5D). Consistent with the *in vitro* data, DUSP14 silencing reduced the expression of stem cell markers (OCT4 and SOX2) in the xenograft tumor tissues (Fig. 5E). Together, the obtained results indicate that DUSP14 exerts a critical role in supporting the growth and stemness of NSCLC cells.

4. Discussion

NSCLC is a significant reason for tumor-related mortality, despite advancements during early diagnosis and treatment. The prognosis for this disease remains unfavorable [18]. Therefore, it is crucial to identify novel molecular markers and gain insights into the key mechanisms driving NSCLC progression in order to develop effective treatments.

It has been previously indicated that the Dual-specificity phosphatase (DUSP) family exhibits abnormal expression in human cancers, including pancreatic cancer, melanoma [19], and glioblastoma [20]. To date, more than forty DUSPs have been identified [21], many of which have been reported to regulate MAPK/ERK signaling pathways, controlling cell proliferation, differentiation, as well as immune responses [22,23]. For instance, higher expression of DUSP9 has been observed in hepatocellular carcinoma and breast cancer, which is associated with the prognosis of patients [24,25]. DUSP22 is downregulated in prostate cancer and it suppresses cancer cell proliferation through targeting EGFR/ERK [26]. As a novel member of the DUSP family, DUSP14 was initially reported to not include the kinase interaction sequence. However, later studies showed that DUSP14 could also regulate the activity of cell cycle-related kinases, such as MAPK, ERKs, and JNKs [27,28]. In pancreatic cancer, DUSP14 was reported to be overexpressed, and its high expression correlates with advanced tumor stages and metastasis, indicating its potential as a prognostic biomarker [16]. In the present study, we also reported the upregulation of DUSP14 in NSCLC tumor tissues and cell lines. Additionally, elevated DUSP14 expression is correlated with a poor prognosis in lung cancer patients. Our findings suggest that DUSP14 upregulation makes contribution to the malignant progression of NSCLC.

Proliferation, tissue invasion, and stemness are crucial processes that drive cancer progression and metastasis [29]. Stemness is closely related to acquired resistance. The upregulation of stemness-related proteins SOX2 and OCT4 modulates resistance to chemotherapeutic drugs, such as paclitaxel and gefitinib [30,31]. Our data suggest that high expression of DUSP14 is required to sustain the aggressiveness and stemness in NSCLC cells, since the knockdown of DUSP14 reduced cell growth, invasion, sphere-forming ability, as well as the protein levels of stem cell markers (SOX2 and OCT4). Consistently, NSCLC cells with DUSP14 knockdown showed impaired tumor growth *in vivo* and exhibited reduced expression of stemness markers (SOX2 and OCT4). These findings imply that DUSP14 overexpression fosters the malignancy of NSCLC cells, and DUSP14 may act as a therapeutic target in NSCLC treatment.

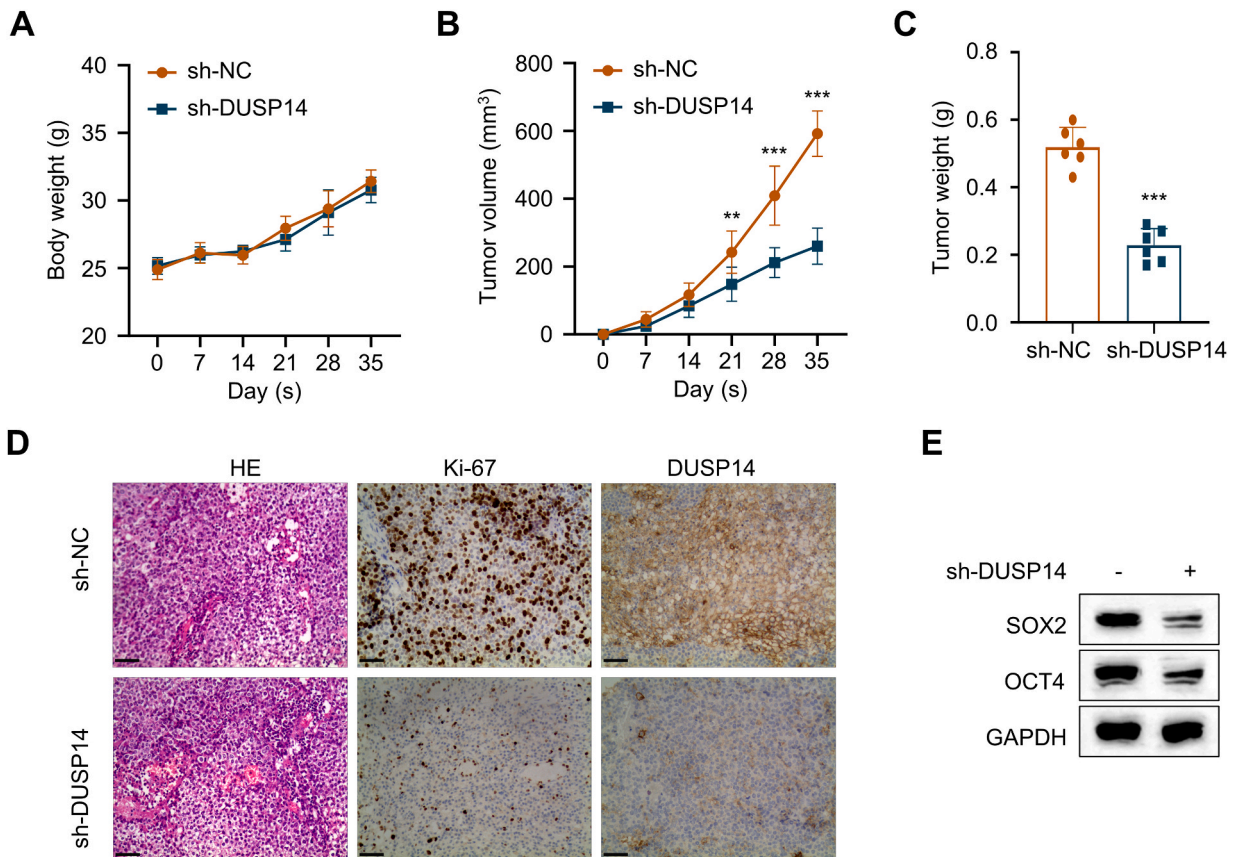


**Fig. 5. DUSP14 is required of the tumor growth of A549 cells *in vivo*.** A549 cells stably expressing sh-NC or sh-DUSP14 were injected into BALB/c nude mice. **A.** The body weight and **B.** the tumor volume were measured every a week for 5 weeks. **C.** The xenograft weight was recorded. **D.** H&E staining and immunohistochemistry of Ki-67 and DUSP14 in tumor tissues (scale bar = 50 μm). **E.** Western bot analysis of SOX2 and OCT4 protein levels in the subcutaneous tumor tissues. \*\**p* < 0.01, \*\*\**p* < 0.001, in relative to sh-NC.

The miRNA refers to a type of single-stranded non-coding RNA regulating gene expression through binding to the 3'UTR region of target mRNAs [32]. An increasing number of evidence indicates that the deregulation of miRNAs is indicated in the initiation and progression of NSCLC [8]. Previous studies have shown that miR-9 and miR-155 can target DUSP14 in metastatic breast cancer [33]. In cerebral ischemia/reperfusion (I/R) injury, miR-155-5p exacerbates tissue injury by downregulating DUSP14 [15]. In contrast, inhibiting miR-217 activity protects against myocardial I/R injury through relieving the repression of DUSP14 expression [34]. However, the specific miRNA that targets DUSP14 in NSCLC has not been identified. This study performed miRNA prediction and miRNA mimic transfection experiment to identify miR-199a-5p as an upstream regulator of DUSP14. In clinical samples, miR-199a-5p levels were notably lower in NSCLC tumor tissues, and there was a negative correlation between miR-199a-5p and DUSP14 expression. Furthermore, forced DUSP14 expression could rescue the inhibitory effect of miR-199a-5p mimic on NSCLC cells. Our data indicate that the downregulation of miR-199a-5p in NSCLC tumor cells lead to DUSP14 overexpression, which facilitates the malignant progression of NSCLC.

Four miRNAs have been identified in the miR-199 family, namely miR-199a-5p/-3p and miR-199b-5p/-3p. These members can function as either oncogenes or suppression genes in different malignancies [35]. For instance, the level of miR-199b-3p was elevated in colon cancer, and its inhibition increased the anti-tumor effects of chemotherapeutic cetuximab [36]. Another study indicated that miR-199a-3p inhibited cell growth and the epithelial-to-mesenchymal transition (EMT) process in Cutaneous squamous cell carcinoma through targeting Ras-associated protein B2 (RAP2B) [37]. According to our results, the transfection of miR-199a-5p mimic reduced the proliferation, invasion and stemness of NSCLC cells. Importantly, the anti-cancer effect of the miR-199a-5p mimic could be at least partially counteracted by overexpressing DUSP14. Together, our data indicate that targeting the miR-199a-5p/DUSP14 axis provides a strategy to curb the malignant progression of NSCLC.

## 5. Conclusion

The present article analyzed multifunctional effects of miR-199a-5p/DUSP14 axis on dictating malignant characteristics of NSCLC cells. According to the results, DUSP14 was up-regulated, whereas miR-199a-5p was down-regulated in NSCLC tumor samples. Silencing DUSP14 and introducing miR-199a-5p showed similar inhibitory effects on NSCLC cell growth, invasion, and stemness. Our findings imply that targeting miR-199a-5p/DUSP14 axis is the potential way to hinder NSCLC progression.

## Ethics approval and consent to participate

Collection of samples used in this study was approved by the Ethics Committee of Yibin Second People's Hospital. (20151216). Every patient provided the informed consent.

Each animal experimental procedure gained approval from Animal Ethics Committee of Yibin Second People's Hospital. The experimental protocol was performed in accordance with the relevant guidelines and regulations of the Basel Declaration. The study is reported in accordance with ARRIVE guidelines (<https://arriveguidelines.org>).

## Consent for publication

All cases provided the informed consent.

## Data availability statement

Data used in the present work can be obtained from corresponding author on request via email.

## Funding

The authors received no financial support for the research authorship and/or publication of this article.

## CRediT authorship contribution statement

**Ying Zheng:** Writing – original draft, Methodology, Investigation, Formal analysis, Data curation, Conceptualization. **Chaokun Yang:** Writing – original draft, Data curation, Conceptualization. **Shaoqiang Xie:** Writing – original draft, Methodology, Data curation. **Desheng Liu:** Writing – original draft, Methodology, Conceptualization. **Hui Wang:** Data curation. **Jinxin Liu:** Writing – original draft, Supervision, Methodology, Data curation, Conceptualization.

## Declaration of competing interest

The authors declare that they have no known competing financial interests or personal relationships that could have appeared to influence the work reported in this paper.

## Acknowledgements

Not applicable.

## Abbreviation

NSCLC Non-small cell lung cancer  
 MicroRNAs miRNAs  
 The dual-specificity phosphatases DUSPs  
 Lung squamous cell carcinoma LSCC  
 Fetal bovine serum FBS  
 Short hairpin RNA shRNA  
 Cell Counting Kit-8 CCK-8  
 Negative control NC  
 Hematoxylin and eosin H&E  
 3' untranslated region 3'UTR  
 MAP-kinase phosphatase 6 MKP6  
 Ischemia/reperfusion I/R  
 Epithelial-to-mesenchymal transition EMT  
 Ras-associated protein B2 RAP2B

## Appendix A. Supplementary data

Supplementary data to this article can be found online at <https://doi.org/10.1016/j.heliyon.2024.e29102>.

## References

- [1] N. Duma, R. Santana-Davila, J.R. Molina, Non-small cell lung cancer: epidemiology, screening, diagnosis, and treatment, *Mayo Clin. Proc.* 94 (2019) 1623–1640, <https://doi.org/10.1016/j.mayocp.2019.01.013>.
- [2] R. Ye, R. Tang, S. Gan, R. Li, Y. Cheng, L. Guo, C. Zeng, Y. Sun, New insights into long non-coding RNAs in non-small cell lung cancer, *Biomed. Pharmacother.* 131 (2020) 110775, <https://doi.org/10.1016/j.biopha.2020.110775>.
- [3] T. Treiber, N. Treiber, G. Meister, Publisher Correction: regulation of microRNA biogenesis and its crosstalk with other cellular pathways, *Nat. Rev. Mol. Cell Biol.* 20 (2019) 321, <https://doi.org/10.1038/s41580-019-0106-6>.
- [4] D. Rosolen, E. Nunes-Souza, R. Marchi, M.V. Tofolo, V.C. Antunes, F.C.B. Berti, A.S. Fonseca, L.R. Cavalli, MiRNAs action and impact on mitochondria function, metabolic reprogramming and chemoresistance of cancer cells: a systematic review, *Biomedicines* 11 (2023), <https://doi.org/10.3390/biomedicines11030693>.
- [5] R. Cuttano, M.K. Afanga, F. Bianchi, MicroRNAs and drug resistance in non-small cell lung cancer: where are we now and where are we going, *Cancers* 14 (2022), <https://doi.org/10.3390/cancers14235731>.
- [6] J. Rhim, W. Baek, Y. Seo, J.H. Kim, From molecular mechanisms to therapeutics: understanding MicroRNA-21 in cancer, *Cells* 11 (2022), <https://doi.org/10.3390/cells11182791>.
- [7] G. Romano, P. Le, G. Nigita, M. Saviana, L. Micalo, F. Lovat, D. Del Valle Morales, H. Li, P. Nana-Sinkam, M. Acunzo, A-to-I edited miR-411-5p targets MET and promotes TKI response in NSCLC-resistant cells, *Oncogene* (2023), <https://doi.org/10.1038/s41388-023-02673-y>.
- [8] K. Kielbowski, K. Ptaszynski, J. Wojcik, M.E. Wojtys, The role of selected non-coding RNAs in the biology of non-small cell lung cancer, *Adv. Med. Sci.* 68 (2023) 121–137, <https://doi.org/10.1016/j.advms.2023.02.004>.
- [9] X. Liu, X. Wang, B. Chai, Z. Wu, Z. Gu, H. Zou, H. Zhang, Y. Li, Q. Sun, W. Fang, et al., miR-199a-3p/5p regulate tumorigenesis via targeting Rheb in non-small cell lung cancer, *Int. J. Biol. Sci.* 18 (2022) 4187–4202, <https://doi.org/10.7150/ijbs.70312>.
- [10] Q. Hua, M. Jin, B. Mi, F. Xu, T. Li, L. Zhao, J. Liu, G. Huang, LINC01123, a c-Myc-activated long non-coding RNA, promotes proliferation and aerobic glycolysis of non-small cell lung cancer through miR-199a-5p/c-Myc axis, *J. Hematol. Oncol.* 12 (2019) 91, <https://doi.org/10.1186/s13045-019-0773-y>.
- [11] X. Yang, Y. Zheng, J. Tan, R. Tian, P. Shen, W. Cai, H. Liao, MiR-199a-5p-HIF-1 $\alpha$ -STAT3 positive feedback loop contributes to the progression of non-small cell lung cancer, *Front. Cell Dev. Biol.* 8 (2020) 620615, <https://doi.org/10.3389/fcell.2020.620615>.
- [12] Y. Li, D. Wang, X. Li, Y. Shao, Y. He, H. Yu, Z. Ma, MiR-199a-5p suppresses non-small cell lung cancer via targeting MAP3K11, *J. Cancer* 10 (2019) 2472–2479, <https://doi.org/10.7150/jca.29426>.
- [13] Z. Zandi, B. Kashani, Z. Alishahi, A. Pourbagheri-Sigaroodi, F. Esmaeili, S.H. Ghaffari, D. Bashash, M. Momeny, Dual-specificity phosphatases: therapeutic targets in cancer therapy resistance, *J. Cancer Res. Clin. Oncol.* 148 (2022) 57–70, <https://doi.org/10.1007/s00432-021-03874-2>.
- [14] C.Y. Li, Q. Zhou, L.C. Yang, Y.H. Chen, J.W. Hou, K. Guo, Y.P. Wang, Y.G. Li, Dual-specificity phosphatase 14 protects the heart from aortic banding-induced cardiac hypertrophy and dysfunction through inactivation of TAK1-P38MAPK/JNK1/2 signaling pathway, *Basic Res. Cardiol.* 111 (2016) 19, <https://doi.org/10.1007/s00395-016-0536-7>.
- [15] Y. Shi, K. Li, K. Xu, Q.H. Liu, MiR-155-5p accelerates cerebral ischemia-reperfusion injury via targeting DUSP14 by regulating NF- $\kappa$ B and MAPKs signaling pathways, *Eur. Rev. Med. Pharmacol. Sci.* 24 (2020) 1408–1419, <https://doi.org/10.26355/eurrev.202002.20198>.
- [16] Y. Wei, G. Wang, C. Wang, Y. Zhou, J. Zhang, K. Xu, Upregulation of DUSP14 affects proliferation, invasion and metastasis, potentially via epithelial-mesenchymal transition and is associated with poor prognosis in pancreatic cancer, *Cancer Manag. Res.* 12 (2020) 2097–2108, <https://doi.org/10.2147/CMAR.S240040>.
- [17] Y. Guo, Y. He, Comprehensive analysis of the expression of SLC30A family genes and prognosis in human gastric cancer, *Sci. Rep.* 10 (2020) 18352, <https://doi.org/10.1038/s41598-020-75012-w>.
- [18] D.S. Ettinger, D.E. Wood, D.L. Aisner, W. Akerley, J.R. Bauman, A. Bharat, D.S. Bruno, J.Y. Chang, L.R. Chirieac, M. DeCamp, et al., NCCN guidelines(R) insights: non-small cell lung cancer, version 2.2023, *J. Natl. Compr. Cancer Netw.* 21 (2023) 340–350, <https://doi.org/10.6004/jnccn.2023.0020>.
- [19] M.K. Singh, S. Altameemi, M. Lares, M.A. Newton, V. Setaluri, Role of dual specificity phosphatases (DUSPs) in melanoma cellular plasticity and drug resistance, *Sci. Rep.* 12 (2022) 14395, <https://doi.org/10.1038/s41598-022-18578-x>.

- [20] J.W. Park, G. Wollmann, C. Urbiola, B. Fogli, T. Florio, S. Geley, L. Klimaschewski, Sprouty2 enhances the tumorigenic potential of glioblastoma cells, *Neuro Oncol.* 20 (2018) 1044–1054, <https://doi.org/10.1093/neuonc/noy028>.
- [21] A. Quintanal-Villalonga, J.M. Chan, H.A. Yu, D. Pe'er, C.L. Sawyers, T. Sen, C.M. Rudin, Lineage plasticity in cancer: a shared pathway of therapeutic resistance, *Nat. Rev. Clin. Oncol.* 17 (2020) 360–371, <https://doi.org/10.1038/s41571-020-0340-z>.
- [22] M.H. Chen, H.C. Chuang, Y.C. Yeh, C.T. Chou, T.H. Tan, Dual-specificity phosphatases 22-deficient T cells contribute to the pathogenesis of ankylosing spondylitis, *BMC Med.* 21 (2023) 46, <https://doi.org/10.1186/s12916-023-02745-6>.
- [23] B.E. Sanders, T.M. Yamamoto, A. McMellen, E.R. Woodruff, A. Berning, M.D. Post, B.G. Bitler, Targeting DUSP activity as a treatment for high-grade serous ovarian carcinoma, *Mol. Cancer Therapeut.* 21 (2022) 1285–1295, <https://doi.org/10.1158/1535-7163.MCT-21-0682>.
- [24] K. Chen, A. Gorgen, A. Ding, L. Du, K. Jiang, Y. Ding, G. Sapisochin, A. Ghanekar, Dual-specificity phosphatase 9 regulates cellular proliferation and predicts recurrence after surgery in hepatocellular carcinoma, *Hepatol Commun* 5 (2021) 1310–1328, <https://doi.org/10.1002/hep4.1701>.
- [25] T. Jimenez, A. Barrios, A. Tucker, J. Collazo, N. Arias, S. Fazel, M. Baker, M. Halim, T. Huynh, R. Singh, et al., DUSP9-mediated reduction of pERK1/2 supports cancer stem cell-like traits and promotes triple negative breast cancer, *Am. J. Cancer Res.* 10 (2020) 3487–3506.
- [26] C. Marie-Claire, N. Benturquia, A. Lundqvist, C. Courtin, F. Noble, Characteristics of dual specificity phosphatases mRNA regulation by 3,4-methylenedioxy-methamphetamine acute treatment in mice striatum, *Brain Res.* 1239 (2008) 42–48, <https://doi.org/10.1016/j.brainres.2008.08.050>.
- [27] H.C. Chuang, T.H. Tan, MAP4K family kinases and DUSP family phosphatases in T-cell signaling and systemic lupus erythematosus, *Cells* 8 (2019), <https://doi.org/10.3390/cells8111433>.
- [28] C.Y. Yang, L.L. Chiu, T.H. Tan, TRAF2-mediated Lys63-linked ubiquitination of DUSP14/MKP6 is essential for its phosphatase activity, *Cell. Signal.* 28 (2016) 145–151, <https://doi.org/10.1016/j.cellsig.2015.10.017>.
- [29] R. Zhang, Z. Meng, X. Wu, M. Zhang, Z. Piao, T. Jin, PD-L1/p-STAT3 promotes the progression of NSCLC cells by regulating TAM polarization, *J. Cell Mol. Med.* 26 (2022) 5872–5886, <https://doi.org/10.1111/jcmm.17610>.
- [30] Y. Huang, X. Wang, R. Hu, G. Pan, X. Lin, SOX2 regulates paclitaxel resistance of A549 non-small cell lung cancer cells via promoting transcription of CIC-3, *Oncol. Rep.* 48 (2022), <https://doi.org/10.3892/or.2022.8396>.
- [31] Y. Zhou, L. Wang, Z. Sun, J. Zhang, X. Wang, Targeting c-kit inhibits gefitinib resistant NSCLC cell growth and invasion through attenuations of stemness, EMT and acquired resistance, *Am. J. Cancer Res.* 10 (2020) 4251–4265.
- [32] A.M. Harrandah, R.A. Mora, E.K.L. Chan, Emerging microRNAs in cancer diagnosis, progression, and immune surveillance, *Cancer Lett.* 438 (2018) 126–132, <https://doi.org/10.1016/j.canlet.2018.09.019>.
- [33] V. Kia, M. Paryan, Y. Mortazavi, A. Biglari, S. Mohammadi-Yeganeh, Evaluation of exosomal miR-9 and miR-155 targeting PTEN and DUSP14 in highly metastatic breast cancer and their effect on low metastatic cells, *J. Cell. Biochem.* 120 (2019) 5666–5676, <https://doi.org/10.1002/jcb.27850>.
- [34] Y. Li, L. Fei, J. Wang, Q. Niu, Inhibition of miR-217 protects against myocardial ischemia-reperfusion injury through inactivating NF-kappaB and MAPK pathways, *Cardiovasc Eng Technol* 11 (2020) 219–227, <https://doi.org/10.1007/s13239-019-00452-z>.
- [35] Q. Wang, B. Ye, P. Wang, F. Yao, C. Zhang, G. Yu, Overview of microRNA-199a regulation in cancer, *Cancer Manag. Res.* 11 (2019) 10327–10335, <https://doi.org/10.2147/CMAR.S231971>.
- [36] H. Han, Y. Li, W. Qin, L. Wang, H. Yin, B. Su, X. Yuan, miR-199b-3p contributes to acquired resistance to cetuximab in colorectal cancer by targeting CRIM1 via Wnt/beta-catenin signaling, *Cancer Cell Int.* 22 (2022) 42, <https://doi.org/10.1186/s12935-022-02460-x>.
- [37] M. Masalha, T. Meningher, A. Mizrahi, A. Barzilai, H. Tabibian-Keissar, D. Gur-Wahnon, I.Z. Ben-Dov, J. Kapenhas, J. Jacob-Hirsch, R. Leibowitz, et al., MiR-199a-3p induces mesenchymal to epithelial transition of keratinocytes by targeting RAP2B, *Int. J. Mol. Sci.* 23 (2022), <https://doi.org/10.3390/ijms232315401>.